Available online at www.sciencedirect.com
SCIENCE DIRECT
ELSEVIER
International Journal of Mass Spectrometry 252 (2006) 180–188
International Journal of Mass Spectrometry
www.elsevier.com/locate/ijms

Characterisation of DEFB107 by mass spectrometry: Lessons from an anti-antimicrobial defensin

Bryan J. McCullough [a], Hayden Eastwood [a], Dave J. Clark [a], Nick C. Polfer [a,1], Dominic J. Campopiano [a], Julia A Dorin [b], Alison Maxwell [b], Ross J. Langley [c], John R.W. Govan [c], Summer L. Bernstein [d], Michael T. Bowers [d], Perdita E. Barran [a,*]

[a] *School of Chemistry, University of Edinburgh, West Mains Road, Edinburgh EH9 3JJ, UK*
[b] *MRC Human Genetics Unit, Western General Hospital, Edinburgh, UK*
[c] *Medical Microbiology, School of Medicine, University of Edinburgh, UK*
[d] *Department of Chemistry and Biochemistry, UCSB, USA*

Received 12 January 2006; received in revised form 16 January 2006; accepted 17 January 2006
Available online 29 March 2006

Abstract

Mammalian defensins are small endogenous cationic proteins which form a class of antimicrobial peptides that is part of the innate immune response of all mammalian species [R. Lehrer, Nat. Rev. Microbiol. 2 (9) (2004) 727; T. Ganz, R.I. Lehrer, Curr. Opin. Immunol. 6 (4) (1994) 584] [1,2]. We have developed mass spectrometry based strategies for characterising the structure–activity relationship of defensins [D.J. Campopiano, D.J. Clarke, N.C. Polfer, P.E. Barran, R.J. Langley, J.R.W. Govan, A. Maxwell, J.R. Dorin, J. Biol. Chem. 279 (47) (2004) 48671; P.E. Barran, N.C. Polfer, D.J. Campopiano, D.J. Clarke, P.R.R. Langridge-Smith, R.J. Langley, J.R.W. Govan, A. Maxwell, J.R. Dorin, R.P. Millar, M.T. Bowers, Int. J. Mass Spectrom. 240 (2005) 273] [3,4], and here we present data obtained from a five cysteine containing β-defensin, DEFB107. The synthetic product of this human defensin exists with a glutathione capping group, its oxidation state and disulphide connectivity have been determined via accurate mass measurements and peptide mass mapping respectively, and despite possessing three disulphide bridges, it does not fit the β-defensin canonical motif. With the use of molecular modelling, we have generated candidate geometries to discern the influence of disulphide bridging on the overall tertiary structure of DEFB107. These are compared with experimental results from ion mobility measurements.

Defensins display activity against a wide variety of pathogens including both gram-negative and gram-positive bacteria. Their mechanism of mode of action is unknown, but is believed to involve defensin aggregation at cell surfaces, followed by cell permeabilisation and hence death. To probe this mechanism, the localisation of DEFB107 in synthetic vesicles was studied using H/D exchange and mass spectrometry. The results obtained are used to analyse the antimicrobial activity of DEFB107.

Keywords: DEFB107; Mass spectrometry; β-Defensin; Ion mobility; Molecular modelling

1. Introduction

Mammals have evolved an exceptionally sophisticated defense system to ward off attack from incoming micro-organisms. As you read this, each square centimeter of your skin will contain between 100 and 1000 bacteria; this totals to an average of 10^{12} over your entire skin. In addition you will have 10^{10} in your mouth and 10^{14} in your gastrointestinal tract, this latter portion weighing almost 1 g! A great number of these are potentially pathogenic, and given that the average bacterium has a doubling time of 20 min it is clear that our immune system must work exceptionally fast to ward off this constant threat. The immediate response to this bacterial onslaught is termed 'innate immunity', and the major players in this are antimicrobial peptides (AMPs) [1].

Defensins are one of the more ubiquitous families of AMPs; found in a wide variety of species, from humans to plants. They are small (∼30–45 residues, 3–4 kDa), cationic and cysteine rich. One of the more intriguing characteristics of defensins is their lack of sequence homology i.e. apart from the cysteines and cationic residues there is little or no sequence conservation

* Corresponding author.
E-mail address: perdita.barran@ed.ac.uk (P.E. Barran).
[1] Present address: FOM Institute 'Rijnhuizen', Postbus 1207, Edisonbaan 14, 3430 BE Nieuwegein, The Netherlands.

1387-3806/$ – see front matter © 2006 Elsevier B.V. All rights reserved.
doi:10.1016/j.ijms.2006.01.054

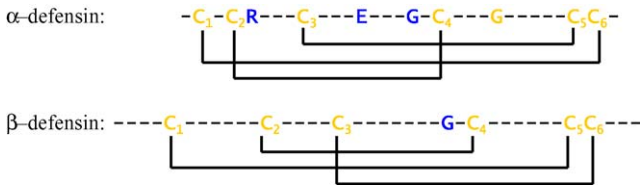

Fig. 1. The canonical disulphide bridging pattern in α- and β-defensins.

Fig. 2. Sequences for DEFB107 and Defr1.

from one defensin to the next. This property may account for the broad spectrum of activity exhibited by different defensins; some are active against gram-negative bacteria, some are active against gram-positive bacteria [5]. The mature peptides are characterised by the presence of six, conserved cysteine residues which have a propensity to form disulphide bridges (both intra and inter molecular), the presence of which is thought key to the structure–activity relationship of these peptides [6].

Defensins are divided into two categories, α-defensins and β-defensins, based on their gene location, sites of expression and on their pattern of intra-molecular disulphide linkages. The canonical disulphide bridging pattern between the cysteine residues for the two types of defensin is shown in Fig. 1 and whilst for all six cysteine defensins characterised to date these connectivity's hold, the biological purpose of these specific topologies remains to be elucidated. Lu has engineered different disulfide bridging patterns into HBD3 and notes that its bactericidal activity in vitro, is not affected by changing this canonical connectivity [7].

Recently, we have become interested in the characterisation of a number of newly identified β-defensins [3,4] from genome database mining. This paper focuses on the human defensin DEFB107. Its cysteine spacing and chromosomal location are consistent with it being a member of the β-defensin family and a phylogenetic tree [8] reveals it as being the ortholgue of the murine β-defenisn defb13. Despite this, DEFB107 possesses only five cysteines (its sequence is shown in Fig. 2). The codon for the first cysteine (CYS1) has undergone a single nucleotide change that results in an amino acid residue change to serine (SER).

The functional consequence for this divergence to a peptide containing an odd number of cysteines is unclear. Defr1, a murine β-defensin [9] also is encoded with five cysteines, and we have determined that it is found as a disulphide bridged dimer which demonstrates very high activity against a broad range of both gram-positive and gram-negative bacteria [3,9].[2] We embarked on the present study of DEFB107 to further classify five cysteine defensins.

[2] K. Taylor, B.J. McCullough, D.C. Clarke, R.J. Langley, J.R. Dorin, P.E. Barran, D.C. Campopiano, J.G.W. Govan, Unpublished data.

The mechanism of action of defensins is not completely understood, although it certainly involves permeabilistion of the cell membrane. Two general models of permeabilisation of cells by AMPs have been suggested [10]:

1. *Carpet model*: Wherein several molecules sit on the surface of the cell bringing about necrosis.
2. *Pore model*: Here the peptide oligomerises and forms a multimeric pore in the cell membrane causing leakage of the cell contents.

It is not yet established which of these mechanisms describes the mode of action of a typical β-defensin. It is possible that some defensins form pores and others demonstrate a less concerted structural attack on cell walls. One way to gain insight into the mechanism of antimicrobial peptides is to study their interaction with artificial membranes. This approach can be used with a variety of physical measurements, including X-ray diffraction, differential scanning calorimetry [11], and internal reflection infrared spectroscopy [12]. Here we employ a novel mass spectrometry based approach to examine the interactions of DEFB107 with proteoliposomes, which has been inspired by the work of Demmers et al. [13]. The techniques described in this paper form a thorough classification of this unusual five cystine defensin and provide some insight to the structure–activity relationship of defensins.

2. Experimental

2.1. Defensin synthesis and native gel electrophoresis

DEFB107 was chemically synthesized using standard solid phase methodology by Albachem Ltd. (Gladsmuir, UK); 1,2-dimyristoyl-*sn*-glycero-3-phosphocholine (DMPC), trifluoroacetic acid (TFA), 2,2,2-trifluoroethanol (TFE), ethanol, ammonium acetate and methanol were obtained from Sigma–Aldrich (Milwaukee, WI).

Electrophoresis of DEFB107 was performed under reduced and non-reduced conditions. Five micrograms of peptide was dissolved in 10 μl of 0.01% acetic acid and 10 μl of 2× sample buffer (Novex Tricine SDS sample buffer LC1676). Reduction of samples was performed by adding 2 μl of 500 mM dithiothreitol (DTT) and incubating at room temperature for 1 h. The entire sample was loaded and run on a 16% Tricine gel (Invitrogen). (Figure S1)

2.2. Accurate mass analysis and disulphide mapping

The oxidation state of DEFB107 (i.e. whether its cysteines are oxidized to form disulphide bridges or present as free cysteines) was determined using a 9.4 T FT-ICR mass spectrometer (Bruker Daltonics, Billerica). All peptides samples were made up at a concentration of 50 μM (50:49:1), MeOH:H_2O:CH_3COOH). Solutions were ionised by nano-electrospray, from gold/palladium coated tips (Proxeon Biosystems).

Enzymatic digestion of the peptide (500 μg/ml) was performed with trypsin (25 μg/ml) in 50 mM MES buffer pH 5.75.

The reaction was maintained at 37 °C for 4 h, before termination by addition of 0.05% TFA. Peptide digests were desalted and concentrated using C18 ZipTip (Millipore). Samples were eluted into 10 μl of a 50:49:1 CH_3CN:H_2O:CH_3COOH solvent mixture, prior to analysis via nanospray ionisation. Peptide mass mapping was conducted using a Q-TOF1 mass spectrometer (Waters).

2.3. Amber force field molecular modelling

All calculations were performed using the AMBER 99 force field within the Amber 8.0 suite of programs [14]. DEFB107 with a glutathione capping group was built using X-leap with four different disulphide connectivity patterns. The glutathione residue was made following the RESP procedure. All amino acids were held at their physiological ionisation states, barring the acidic groups in glutathione which were protonated and the histidine which was neutralised, this confers to the peptide a net charge of 2+. A simulated annealing procedure was employed for an initial gas phase energy minimization of the structures. High temperature dynamics was performed at 800 K followed by dynamics at decreasing temperatures according to an exponential cooling curve. At 0 K the candidate structure is subjected to minimization using a steepest descent approach followed by a conjugate gradient algorithm. The minimized structure is then used as the seed for the next run of high temperature dynamics and for each connectivity, 100 candidate structures were generated. All calculations were performed on a HP Intel P4 3.2 GHz PC running Mandrake 9.2 Linux. The lowest energy structures from this run are those discussed within the text. These structures were viewed and analysed using VMD [15] and collision cross-sections calculated using the projection approximation [16].

2.4. Ion mobility measurements

Ion mobility measurements were made on home-built apparatus which has been described in detail previously [17]. Briefly, DEFB107 was nanosprayed from a 20 μM solution either comprised of 49% water 1% acetic acid and 50% methanol, or an aqueous solution buffered to pH 7.4 using ammonium acetate. Ions pass through an ion funnel and are pulsed into a temperature regulated drift cell filled with helium to a pressure of 5 Torr. Post-drift cell ions are mass analysed using a single quadrapole and arrival time distributions are recorded at the detector for several drift voltages. The mobility (K) of the ion is found via a plot of arrival times versus the pressure of helium divided by the drift voltage. This mobility is used to determine the experimental collision cross-section of the ion (σ) according to Eq. (1) [18]:

$$K = \frac{3e}{16N}\left(\frac{2\pi}{\mu k_B T}\right)^{1/2}\frac{1}{\sigma} \quad (1)$$

where N is the buffer gas number density, T the temperature of the buffer gas, and μ is the reduced mass of the ion and the helium buffer gas.

Experimental cross-sections are compared to those obtained from candidate geometries modelled with the AMBER force field (see below).

2.5. Location of DEFB107 in proteoliposomes

Two hundred and fifty microlitres of DEFB107 (1 mg/ml in water) was freeze dried under vacuum overnight. It was then dissolved in a small volume (250 μl) of TFA and subsequently dried under a stream of nitrogen; this was repeated using TFE. The peptide was re-dissolved in TFE to a concentration of 1 mg/ml, and this solution mixed with a solution of DMPC in methanol (∼5 mg/ml) to give a peptide to lipid ratio of approximately 1:25. The solution was vortexed vigorously and all excess solvent removed under nitrogen at 40 °C (i.e. above the lipid glass transition temperature) to leave a mixed peptide/lipid film. This was dried under vacuum for 24 h prior to hydration in 0.5 ml of ammonium acetate (10 mM, pH 7.5) at 40 °C. Large unilamellar vesicles (LUVETs) were prepared by extrusion through a 0.1 μM membrane (Avanti Polar Lipids Inc., Birmingham, AL). Prior to H/D exchange the LUVETs were preincubated for 30 min at 30 °C. The solution was then 50 times diluted in deuterated ammonium acetate (10 mM, pH 7.5) at 30 °C. At selected time points 10 μl of this solution was transferred into a nanospray tip (Proxeon Biosystems, Denmark) and analysed by MS using a Micromass Q-TOF 1. The dead time between dilution and measurement was 3 min. The desolvation process involved in electrospray ionisation causes the lipids to fall away from the peptide and therefore it is the mass of the uncomplexed peptide which is measured. CID was performed at approx 80 V collision voltage using argon as the collision gas, at a pressure of 10 psi. This will result in multiple collisions.

Increases in deuterium content were calculated using the average m/z values of the undeuterated, partially deuterated and fully deuterated peptide.

2.6. Antimicrobial activity assays

Bacteria were grown to mid-logarithmic phase in Iso-Sensitest growth media and then diluted to 2×10^6 colony-forming units (CFU) per milliliter in 10 mM potassium phosphate containing 1% (v/v) Iso-Sensitest, pH 7.4. Different concentrations of test peptide were incubated in 100 μl of cells at 37 °C for 4 h. Ten-fold serial dilutions of the incubation mixture were plated on Iso-Sensitest plates, at 37 °C. Results are presented in terms of the minimum inhibitory concentration MIC (the concentration of peptide required to fully inhibit bacterial growth). All assays were repeated at least three times and experimental errors were found to be within one doubling dilution.

3. Results and discussion

3.1. Accurate mass and disulphide connectivity

Accurate mass spectrometry was performed to establish the oxidation state of this peptide. The predicted (monoisotopic) mass, based on the sequence (Fig. 2) is 4264.03 Da (assuming 2 disulphide bridges and one free cysteine) however the measured mass was 4571.10 Da corresponding to a mass increase of 307.07. This value fits extremely well with the mass of a

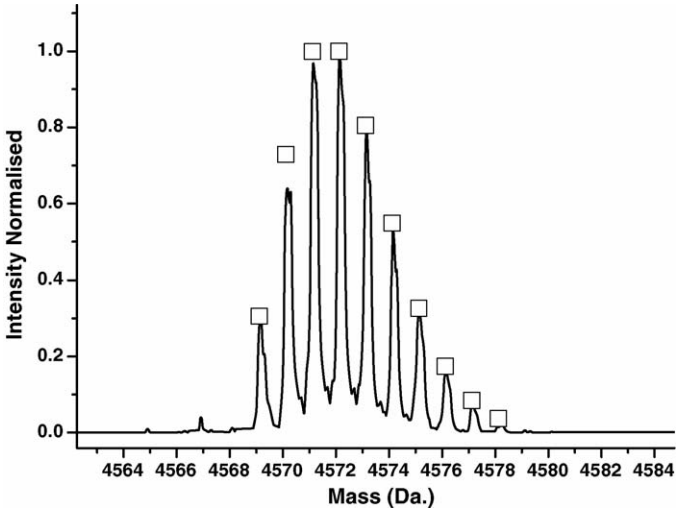

Fig. 3. DEFB107 FT-ICR isotopic envelope. The deconvoluted isotopic envelope from FT-ICR nanospray analysis of oxidized DEFB107. Empty squares correspond to the isotopic envelope expected from a DEFB107 with a glutathionie capping group and all cysteines oxidized i.e. containing three disulfides.

glutathione capping group. Glutathione (GSH) is a tri-peptide comprised of glutamic acid, cysteine, and glycine. GSH is abundant in nature, where it reduces disulfide bonds formed within cytoplasmic proteins. Its presence here however, is due to the synthetic strategy employed. GSH is used as an oxidising agent to assist the formation of disulphide bridges post-synthesis, and since DEFB107 has an *odd* number of cystine residues, a disulphide bridge between the free cysteine and the cysteine on GSH has formed.

Fig. 3 shows the results of our accurate mass analysis. The deconvoluted spectrum produces a well resolved isotopic envelope, onto which we have imposed a simulated isotopic distribution derived from the elemental composition of the fully oxidised peptide along with a glutathione capping group i.e. possessing three disulphide bridges. The simulated and experimental data match exceedingly well. After reduction of the peptide (data not shown) the observed mass was 4268.07, corresponding to DEFB107 with five cysteines, and the loss of the glutathione capping group.

This finding poses the question: on which cysteine(s) is the glutathione group located? and further what are the remaining internal disulphide bridges? Mass spectrometry has been utilised by several groups to elucidate disulphide connectivity's in polypeptides and proteins [19–21]. Table 1 identifies the masses found for the tryptic peptides, and Table 2 lists the 'y' ions obtained on sequencing a precursor doubly charged ion of mass 862.4, fragment 3 in Table 1. These results show that DEFB107 exists as a single isomer with a unique disulphide bridging pattern. CYS4 is not connected to CYS6 [22] (as for the canonical β-defensin) but to CYS5, CYS6 is instead capped by glutathione, this is confirmed by MS/MS analysis where the y2 ion obtained (mass 544.3) corresponds to CK with glutathione attached. As Table 2 shows, sequencing also reveals the results of CID on fragment 3 confirming that that CYS2 is connected to CYS3. The absence of CYS1 in DEFB107 and perhaps the

Table 1
Calculated and observed masses of tryptic fragments (Da) used for determination of disulphide connectivity's for oxidised DEFB107

Fragment number	Sequence	Theoretical mass	Measured mass
1	R	174.11	174.09
2	ALISK	530.34	530.33
3	MEGHCEAECLTFEVK IGGCR AELAPFCCK	1722.71	1722.74
4	Glt	1787.75	1788.23
5	NR	288.15	Not observed

Trypsin digest of the peptide produced fragments which were analysed by ESI-MS.

presence of the GSH capping group has resulted in this distinct and unusual disulphide bridging pattern.

These results contrast with our findings for Defr1 (Fig. 2) which instead of remaining capped by the redox agents used to oxidise synthetic cysteine rich peptides, forms a disulphide bridged dimmer [3]. In addition Defr1 was not observed as a single isomer, and instead presents a mixture of disulphide connectivity's. Disulphide bridge scrambling for synthetically produced defensins has been reported by several groups [7,23], and in particular for defensin related peptides with odd numbers of cysteines both in vitro and from peptides extracted from cells [24], so it is somewhat surprising that DEFB107 folds to a single conformer. It is possible that the bound GSH group chaperones this process.

There is a consensus that defensins form non-covalent aggregates under certain conditions [1], for example HBD1, and HBD2 have been observed as dimers by crystallography [25] and our previous work using both ESI-MS and native gel electrophoresis shows the six cystine variant of Defr1 (Defr1 Y5C) forms a stable non-covalent dimer [3]. Despite DEFB107 not being found as a disulphide bridged dimer, under certain electrospray conditions we were also able to observe it as a low abundance non-covalently bound dimer (data not shown). This species was not however observed with native SDS-PAGE analysis (Figure S1), which suggests that it is only very weakly bound, and perhaps just an artefact of the electrospray process. It can be surmised that DEFB107 with this peculiar fold, has

Table 2
Assignment of S–S connectivity for fragment 3 was determined to be CYS2–CYS4 using CID

Measured mass	Calculated mass for the singly charged ion	Fragment
146.08	146.18	y1
245.15	245.32	y2
374.19	374.44	y3
454.14	454.16	y4
1165.37	1166.62	y10
1268.56	1269.46	y11
703.80 (2+)	1406.60	y12
795.89 (2+)	1592.77	y14
897.135 (2+)	1723.97	$[M+2H]^{2+}$

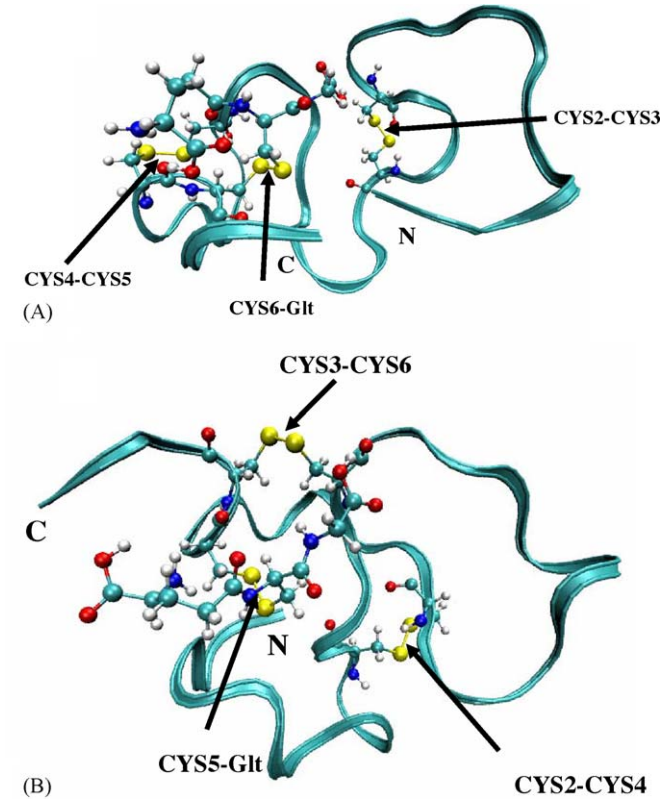

Fig. 4. Calculated low energy gas-phase structures for DEFB107 with A CYS2–CYS3 and CYS4–CYS5 connectivity and glutathione capping CYS6, and B β-defensin connectivity with glutathione capping CYS5. The polypeptide backbone is represented by a light blue ribbon, and the cysteine and glutathione residues shown as CPK structures. (For interpretation of the references to colour in this figure legend, the reader is referred to the web version of the article.)

some aggregation propensity, but far less than has been reported for other defensins.

3.2. Insights into the structure of DEFB107 from molecular modelling and ion mobility

With use of molecular modelling, we have examined structures adopted by DEFB107 when different disulphide topologies are present. In this preliminary study, we have investigated gas phase conformations and used experimental collision cross-sections as an order parameter by which to judge our modelled geometries. Fig. 4 contains two representative low energy structures obtained from our calculations. Fig. 4A shows the disulphide bridge topology found experimentally for synthetic DEFB107, and Fig. 4B is a structure arising from canonical β-defensin disulphide bridging. On first appearance, the two different topologies appear to give similar structures, however closer inspection shows that the CYS2–CYS3 and CYS4–CY5 connectivity will impart much greater conformational flexibility to the molecule, the N and C terminal sections will be able to be quite separate from one another. By leaving all amino acids in their physiological charge states, our calculated gas-phase structures exhibit a large number of salt-bridges formed between the acidic and basic groups. Of course we do not know whether this is the form that we observe this peptide experimentally and indeed we never have observed in solely in a 2+ charge state, instead these calculated structures illustrate the conformational constraints that differing connectivity's impose on the peptide backbone. Since electrostatic interactions are favoured in a solvent free environment, the observed salt bridges are strengthened, however the same effect will increase coulombic repulsion, and this is apparent in our ion mobility data (Table 3) as we increase the number of charges.

Table 3
Experimental collision cross-sections of DEFB107 given in $Å^2$ for all observable charge states when electrosprayed from both a buffered aqueous solution and also from 50:49:1 water:methanol:acetic acid

Charge state (+)	pH 7.4	MeOH:aa:H_2O
3	610.0	
4	648.3	
5	765.7	769.8
6		818.7
7		864.7

One of the most exciting applications of ion mobility mass spectrometry is its ability to discern the intermediate structures occupied by proteins as they unfold. Several studies have been performed to examine the change in cross-section of ions as a function of time [26] and temperature [27] and invariably as a function of charge state. Table 3, which reports the experimental collision cross-sections obtained for DEFB107 at room temperature, is an example of the latter criterion. For every ion only single conformations were distinguishable. As the charge state of the ion increases so too does the collision cross-section, due to coulombic repulsion between increasing numbers of protonated basic residues. Between 3+ and 4+ there is little change in the cross-section, however between 4+ and 5+ there is a rapid increase of nearly 20%, indicating an unfolding event, perhaps involving the N and C terminal regions of the peptide moving away from each other. The rate of increase lessens after this, which suggests that for the higher charge states the polypeptide backbone has opened sufficiently such that the unfolding protein can accommodate the protons more effectively. This data taken in tandem with the disulphide topology elucidated above, shows how important the canonical fold may be to β-defensins.

The connectivities indicated in Fig. 1 result in a conformationally constrained structure, that once oxidised, possesses a tight disulphide knot which will no-longer be able to unfold to any extent. This is illustrated with reference to our calculated conformations. Even with the low 'physiological' charge state of 2+ taken here, and with structures determined from gas-phase calculations, there is a difference between the average cross-sections obtained for the canonical β-defensin topology and that for the extended fold identified here (Table 4). We cannot directly compare the cross-sections obtained for our calculated structures with those observed via ion mobility, since the charge state is lower that the first observed experimentally. However given that the projection approximation becomes less accurate for collision cross-sections for molecules of greater

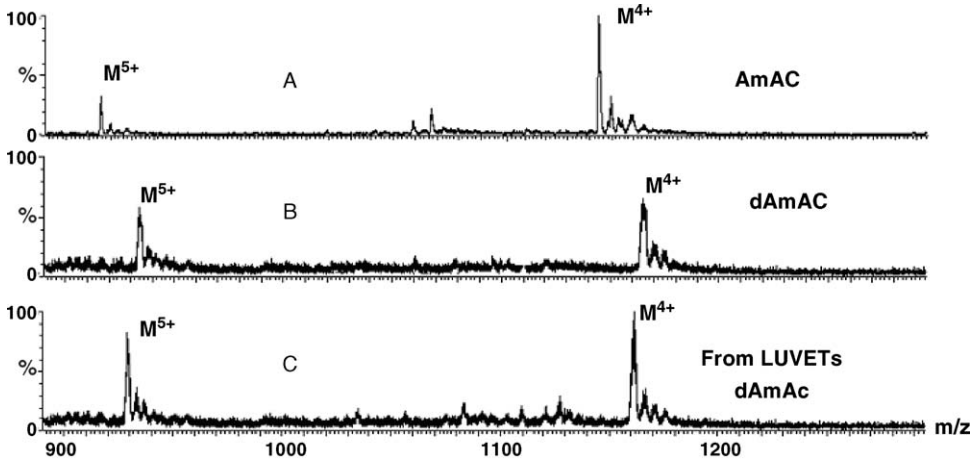

Fig. 5. Mass spectra obtained when investigation the interaction of DEFB107 with proteoliposomes. (A) The major charges states observed (4+ and 5+) when DEFB107 is electrosprayed from 10 mM ammonium acetate (AmAc) (average mass = 4572.05 Da). (B) The same region of the spectrum of DEFB107 obtained following incubation of the LUVETs in deuterated 10 mM ammonium acetate (dAmAc) (average mass = 4638.14 Da, ~66 exchanged). (C) The charge state distribution from obtained when flown from 10 mM dAmAc (average mass = 4649.98 Da, 77 exchanged).

than 200 atoms, the values presented here for the 2+ charge states structures agree remarkably well with what might be extrapolated from the experimental measurements. The geometry for the observed ions at the 3+ charge state could fit with any of the cross-sections found for the different topologies, but the change in collision cross-section as the charge state increases to a far more extended geometry supports our assignment of the CYS2–CYS3 and CYS4–CYS5 connectivities. The overall increase as the charge state range from 3+ to 7+ is from 610.0 to 864.7 $Å^2$, or just over 40%, this compares well with the change reported for a slightly larger protein Ubiqutin where from 4+ to 8+ the average increase in experimental collision cross-section is 50% [28]. Ubiqutin does not posses any disulphide bridges. An inspection of Fig. 4B where we show the fruits of modelling the typical β-defensin fold, is clearly a more compact geometry than that present in Fig. 4A, moreover, the presence of the cross-peptide CYS2–CYS4 and CYS3–CYS6 bridges must always restrict the conformational space of this peptide.

Wu et al. have elegantly demonstrated that disulphide connectivities are not imperative for antimicrobial action when tested in vitro [7] environment, but no one has yet examined the importance of disulphide bridges on the actions of defensins in vivo. Furthermore Wu reports the significance of disulphide bridges on the chemotactic properties of defensins, where a structural motif, which will be conferred by a conserved disulphide bridging pattern will be imperative for specific interactions with a given receptor. It is probable that the disulphide bridges also confer proteolytic resistance to antimicrobial peptides, and indeed this has been shown for α-defensins by Maemoto et al. [29]. In our investigations of several defensins and related peptides, the absence of disulphide bridges renders them much more prone to degragation.[3]

Table 4
Collision cross-sections in $Å^2$ found from low energy calculated geometries for four different disulphide topologies

Connectivity	Average cross-section for lowest 20%	Average cross-section for all
2–4 3–6 5-Glt	596.5 (15.1)	607.6
2–4 3–5 6-Glt	581.9 (8.68)	607.0
2–5 2–4 6-Glt	591.6 (15.0)	608.7
2–3 4–5 6-Glt	614.5 (11.4)	619.7

3.3. Location in proteoliposomes and implications for activity

In 2000 Demmers et al. described a beautiful technique wherein linear peptides which have been designed to interact with the hydrocarbon chains of phospholipids, are incorporated into vesicles and hydrogen deuterium exchange along with mass spectrometry are employed to probe the solvent accessible regions of the polypeptide [13,30]. We have chosen to apply this method to investigate the interaction of defensins with membranes and report here the results of our first investigations. Before considering the extent of HD exchange following incorporation into a LUVET, we ascertained the total amount of HDX that occurs when the peptide is incubated in D_2O.

Mass spectra for DEFB107 analysed under three different conditions are shown in Fig. 5. The average mass, following deconvolution of the charged ion series for each, is given and it can be seen that a mass increase of 78 amu was obtained on spraying from D_2O (Fig. 5B) compared to H_2O (Fig. 5A). This indicates 78 hydrogen atoms have been exchanged for deuterium, which is the maximum number possible and includes all exchangeable side chain hydrogens. This suggests the entire peptide is solvent accessible which is not surprising in light

[3] C. Barran, D. Campopiano, Unpublished results.

Table 5
Antimicrobial activity of oxidized and reduced (red) DEFB107 and Defr1 and Defr1 Y5C (data taken from Campopiano et al. [3])

Organism	Strain	MBC (μg/ml)			
		DEFB107	DEFB107 (red)	Defr1	Defr1 Y5C
Gram-negative					
P. aeruginosa	PAO1	>100	>100	6	50
E. coli	ATCC 25922	>100	>100	8	100
Gram-positive					
S. aureus	ATCC 25923	>100	>100	10	>100
E. faecalis	ATCC 29212	ND	ND	6	100

of the disulphide bridging pattern we have described above. Deconvolution of the data obtained when the peptide had been incubated in the LUVETs for 60 min is shown in Fig. 5C. This results in an increase in mass of only 66 amu. In the presence of the proteoliposome, 11 less hydrogen atoms have exchanged, suggesting part of the defensin is fully protected from deuteration and must be incorporated in the membrane. The stability of this interaction was probed by taking aliquots of the peptide LUVET slurry and analysing them over time. The findings were consistent over 4 days of analysis, the total number of deuteriums incorporated into the peptide never rose above 66 amu with an experimental error on this measurement of ±1. Moreover this value was reached after approximately 1 h and then did not alter. This suggests that a section of DEFB107 is permanently solvent inaccessible due to being encapsulated by the membrane.

In order to determine which part of the peptide is unavailable for exchange, we took a top down sequencing approach. The 4+ charge state of the partially deuterated peptide was isolated and following CID a loss of ∼280 amu from the parent ion was observed. This corresponds to the mass of fully deuterated GSH, following cleavage at the carbon sulphur bond, this apparent lability of the GSH group on CID was also observed when sequencing the peptide to map the disulphide bridges. It is proposed therefore that the glutathione group is fully solvent accessible and hence the C-terminus of DEFB107 has no strong association with the membrane. From this observation, it is tempting to speculate that the N terminal region of the peptide is what interacts with the LUVET bilayer. Examining the peptide sequence (Fig. 2) prior to the first cysteine, there are 11 amino acids, which are unhindered by a disulphide bridge. Three out of the first four amino acids are aliphatic with low hydrophobicities, and would be good candidates for favourable insertion into the hydrocarbon interior of the LUVET bi-layer. The LYS6 and ARG7 basic residues would provide an excellent anchor by forming strong interactions to the negatively charged phosphate head groups preventing the aliphatic tail from emerging. The maximum number of exchangeable hydrogens in the first five amino acids prior to LYS6 is 11, which is extremely close to the initial number here *not* seen to exchange. If ARG7 and LYS6 are responsible for interactions with the phosphate head groups, then it is likely that their exchangeable hydrogens will become solvent accessible over time, which could account for the slight increase in deuterium uptake observed over the first hour of experimental time. So a plausible explanation for the long lived stable interaction of DEFB107 with this artificial cell wall is via the insertion of the first five or six residues of the N terminus. What is remarkable is that once inserted, there they stay. Although only a handful of β-defensin structures have been solved, they present a similar structure. The cystine bridges are involved in a triple β strand, and the N terminal section, including the CYS1 is invariably helical [1,31,32] as it is in α-defensins [27,33]. For defensins which have been identified [34], but have yet to have their structures solved, the N-terminal regions are often more aliphatic and hence may more likely be the region of the peptide involved in membrane interaction. Many antimicrobial and haemolytic peptides do indeed posses a helical structure [35,36], and so it is not surprising that such a motif is found in defensins, and certainly probable that it is involved in membrane disruption.

What is slightly puzzling is why does the DEFB107 peptide remain stuck in our proteoliposome? If defensins are antimicrobial, we would expect that at some point the peptide would burst the vesicle which would be observable because the peptide would then become fully deuterated, but this does not happen. The explanation for this may merely be that these DMPC LUVET's are too simplistic i.e. that they do not accurately represent the complexity of a bacterial cell wall. However, other biophysical studies of antimicrobial peptides employ such simple lipid bilayers and rupture and penetration can be observed. An alternative rationalisation of this experimental data is provided by the antimicrobial killing data for DEFB107 (Table 5). When tested against either gram-positive or gram-negative bacteria, this human defensin exhibits no ability to kill. So is this the fault of the rouge GSH capping group? Apparently not, since no change is seen in the activity assays after reduction and purification of the peptide. Perhaps this is why the defensin remains in the proteoliposomes, it is not able to rupture them, and perhaps in turn this is due to its very low net charge, possessing an almost equal number of basic versus acidic groups it forms many stable internal salt bridges as evidenced by our calculated structures (Fig. 4) and lacks the highly cationic nature of Defr1 (Fig. 2). Of course the question remains why have we evolved this particular peptide?

4. Conclusions

Our findings from DEFB107 contrast with our previous work on Defr1 although together they represent a new class

of five cysteine containing defensins, which do not possess professed canonical connectivity's. The loss of one cysteine means one intra-molecular disulphide bridge is lost i.e. (CYS1–CYS5) leaving a cysteine free to form other bonds.

In the case of DEFB107, the free cysteine is capped with a glutathione group which prevents dimerisation; whereas in Defr1, the free cysteine is found to form an inter-molecular bond to another Defr1 molecule.

The 'preformed' Defr1 aggregate certainly demonstrates considerable antimicrobial activity, which is 10 times higher than its reduced form. By direct contrast as reported here, DEFB107, demonstrates exceptionally low activity against the same panels of bacteria and shows only the slightest tendency to aggregate via mass spectrometry.

So although our findings for Defr1 revealed a putative relationship between covalently led dimerisation and antimicrobial activity, and whilst there is certainly evidence from structural analysis that *some* defensins form dimers, it is not yet clear whether the postulated assembly process by which defensins are antimicrobial agents is initiated by aggregates of a concerted structural form. The absence of activity for DEFB107 coupled with its inability to form a stable non-covalent dimer, supports the general observation that active defensins should posses some propensity to aggregate.

We have described a novel application of LUVET formation and HDX combined with tandem MS which allows us to pinpoint the part of an antimicrobial peptide that interacts with a phosopholipid bi-layer. It appears that the aliphatic and at times helical, N terminus interacts strongly with the membrane, an observation that will influence our design of future novel antimicrobial peptides. The evidence we provide from mapping the disulphide connectivity's along with ion mobility mass spectrometry and molecular modelling allow use to characterise the effect of the disulphide bridges on the conformational space available to this polypeptide. Several questions are thrown up by this analysis, none more imperative than discerning the biological function of DEFB107, the anti-antimicrobial peptide. The methodologies described here represent a new set of tools to be used to characterise the structure and activity of antimicrobial peptides, and our future work will aim them towards increasingly active defensin inspired peptides.

Acknowledgements

This research was supported by the EPSRC (in particular for their award of an Advanced Research Fellowship to PEB and studentships to HE and BJM), the Royal Society, Waters, and the School of Chemistry at the University of Edinburgh. Professor Nick Hastie of the MRC Human Genetics Unit and Dr. Pat Langridge-Smith (Director, Scottish Instrumentation and Resource Centre for Advanced Mass Spectrometry (SIRCAMS) which provided the FT-ICR instrumentation for this work) are also thanked for their continuing support of our work.

Appendix A. Supplementary data

Supplementary data associated with this article can be found, in the online version, at doi:10.1016/j.ijms.2006.01.054.

References

[1] R. Lehrer, Nat. Rev. Microbiol. 2 (9) (2004) 727.
[2] T. Ganz, R.I. Lehrer, Curr. Opin. Immunol. 6 (4) (1994) 584.
[3] D.J. Campopiano, D.J. Clarke, N.C. Polfer, P.E. Barran, R.J. Langley, J.R.W. Govan, A. Maxwell, J.R. Dorin, J. Biol. Chem. 279 (47) (2004) 48671.
[4] P.E. Barran, N.C. Polfer, D.J. Campopiano, D.J. Clarke, P.R.R. Langridge-Smith, R.J. Langley, J.R.W. Govan, A. Maxwell, J.R. Dorin, R.P. Millar, M.T. Bowers, Int. J. Mass Spectrom. 240 (2005) 273.
[5] R.E. Hancock, R. Lehrer, Trends Biotechnol. 16 (2) (1998) 82.
[6] S.H. White, W.C. Wimley, M.E. Selsted, Curr. Opin. Struct. Biol. 5 (4) (1995) 521.
[7] Z. Wu, D.M. Hoover, D. Yang, C. Boulegue, F. Santamaria, J.J. Oppenheim, J. Lubkowski, W. Lu, Proc. Natl. Acad. Sci. U.S.A. 100 (15) (2003) 8880.
[8] C.A. Semple, A. Maxwell, P. Gautier, F.M. Kilanowski, H. Eastwood, P.E. Barran, J.R. Dorin, BMC Evol. Biol. 5 (1) (2005) 32.
[9] G.M. Morrison, M. Rolfe, F.M. Kilanowski, S.H. Cross, J.R. Dorin, Mamm. Genome 13 (8) (2002) 445.
[10] K.A. Brogden, Nat. Rev. Microbiol. 3 (3) (2005) 238.
[11] K. Lohner, E.J. Prenner, Biochim. Biophys. Acta: Biomembr. 1462 (1/2) (1999) 141.
[12] L. Silvestro, P.H. Axelsen, Biophys. J. 79 (3) (2000) 1465.
[13] J. Demmers, J. Haverkamp, A. Heck, R. Koeppe, J. Killian, Proc. Natl. Acad. Sci. U.S.A. 97 (7) (2000) 3189.
[14] D.A. Case, T.A. Darden, T.E. Cheatham III, C.L. Simmerling, J. Wang, R.E. Duke, R. Luo, K.M. Merz, B. Wang, D.A. Pearlman, M. Crowley, S. Brozell, V. Tsui, H. Gohlke, J. Mongan, V. Hornak, G. Cui, P. Beroza, C. Schafmeister, J.W. Caldwell, W.S. Ross, P.A. Kollman, Amber 8, 2004.
[15] W. Humphrey, A. Dalke, K. Schulten, J. Mol. Graphics 14 (1996) 33.
[16] T. Wyttenbach, G. von Helden, J.J. Batka Jr., D. Carlat, M.T. Bowers, J. Am. Soc. Mass Spectrom. 8 (3) (1997) 275.
[17] T. Wyttenbach, P.R. Kemper, M.T. Bowers, Int. J. Mass Spectrom. 212 (1–3) (2001) 13.
[18] E.W. McDaniel, E.A. Mason, Transport Properties of Ions in Gases, Wiley, New York, 1988.
[19] Z.R. Zhou, D.L. Smith, Biomed. Environ. Mass Spectrom. 19 (12) (1990) 782.
[20] J.F. Qi, W. Wu, C.R. Borges, D.H. Hang, M. Rupp, E. Torng, J.T. Watson, J. Am. Soc. Mass Spectrom. 14 (9) (2003) 1032.
[21] J.J. Gorman, T.P. Wallis, J.J. Pitt, Mass Spectrom. Rev. 21 (3) (2002) 183.
[22] We have chosen to stick with the prevalent numbering for cysteines in defensins. Therefore.
[23] P.A. Raj, K.J. Antonyraj, T. Karunakaran, Biochem. J. 347 (Pt 3) (2000) 633.
[24] M.W. Hornef, K. Putsep, J. Karlsson, E. Refai, M. Andersson, Nat. Immunol. 5 (2004) 836.
[25] D.M. Hoover, O. Chertov, J. Lubkowski, J. Biol. Chem. 276 (42) (2001) 39021.
[26] E.R. Badman, C.S. Hoaglund-Hyzer, D.E. Clemmer, Anal. Chem. 73 (24) (2001) 6000.
[27] D.E. Clemmer, R.R. Hudgins, M.F. Jarrold, J. Am. Chem. Soc. 117 (40) (1995) 10141.
[28] J.W. Li, J.A. Taraszka, A.E. Counterman, D.E. Clemmer, Int. J. Mass Spectrom. 187 (1999) 37.
[29] A. Maemoto, X. Qu, K.J. Rosengren, H. Tanabe, A. Henschen-Edman, D.J. Craik, A.J. Ouellette, J. Biol. Chem. 279 (42) (2004) 44188.
[30] J. Demmers, J. Haverkamp, A. Heck, R. Koeppe, J. Killian, Biophys. J. 78 (1) (2000) 326A.

[31] M.V. Sawai, H.P. Jia, L. Liu, V. Aseyev, J.M. Wiencek, P.B. McCray Jr., T. Ganz, W.R. Kearney, B.F. Tack, Biochemistry 40 (13) (2001) 3810.
[32] M.E. Selsted, S.S. Harwig, J. Biol. Chem. 264 (7) (1989) 4003.
[33] Z. Wu, B. Ericksen, K. Tucker, J. Lubkowski, W. Lu, J. Peptides Res. 64 (3) (2004) 118.
[34] C.A.M. Semple, A. Maxwell, P. Gautier, F.M. Kilanowski, H. Eastwood, P.E. Barran, J.R. Dorin, BMC Evol. Biol. (2005) 5.
[35] Y. Shai, Biochim. Biophys. Acta: Biomembr. 1462 (1/2) (1999) 55.
[36] A. Giangaspero, L. Sandri, A. Tossi, Eur. J. Biochem. 268 (21) (2001) 5589.